Influence of Irradiation Temperature on Void Swelling in NiCoFeCrMn and NiCoFeCrPd

Tai-ni Yang[1], Chenyang Lu[1*], Gihan Velisa[2], Ke Jin[2], Pengyuan Xiu[1], Yanwen Zhang[2,3], Hongbin Bei[2] and Lumin Wang[1,4*]

[1]*Department of Nuclear Engineering and Radiological Sciences, University of Michigan, Ann Arbor, Michigan 48109, United States*
[2]*Materials Science and Technology Division, Oak Ridge National Laboratory, Oak Ridge, TN, 37831, United States*
[3]*Department of Materials Science and Engineering, University of Tennessee, Knoxville, TN, 37996, United States*
[4]*Department of Materials Science Engineering, University of Michigan, Ann Arbor, Michigan 48109, United States*

*To whom correspondence should be addressed. Email: lmwang@umich.edu
chenylu@umich.edu

Abstract

Using ion irradiation and transmission electron microscopy, temperature dependent void swelling and dislocation loop evolution in equiatomic NiCoFeCrMn and NiCoFeCrPd high entropy alloys were investigated. Voids were observed in all tested conditions. An order higher of swelling was observed in both HEAs as temperature increased from 420 to 580℃. Alloying with Pd was found to have a stronger suppression effect on void and dislocation loop growth than alloying with Mn. Possible contributions to the swelling resistance were explored, including localized lattice distortion and higher defect migration barrier in NiCoFeCrPd. Additionally, no phase decomposition was observed in either alloy.

Keywords: Ion irradiation, Temperature dependent void swelling, High-entropy alloys, Transmission electron microscope (TEM)

Main body

High-entropy alloys (HEAs) are loosely defined as multi-element solid solutions composed of five or more principal elements in equimolar or near-equimolar ratios [1]. Such material systems have emerged recently due to their excellent mechanical properties, including high tensile strength, ductility, good thermal stability, and fracture toughness [2-4]. HEAs have a relatively simple crystal structure, such as face centered cubic (fcc) or body centered cubic (bcc). This study will focus on the enhanced irradiation resistance of fcc structured HEAs, which have been demonstrated in various temperature regimes, such as cryogenic temperature (16K) [5], room temperature [6-11], and elevated temperatures [12-15]. The enhanced resistance has been attributed to the complex intrinsic transport properties of HEAs, where the increased compositional complexity of HEAs can reduce the effective interstitial mobility and enhance the vacancy-interstitial recombination.

Although favorable radiation resistance has been demonstrated on several HEAs, systematic studies of the swelling behavior on HEAs irradiate at elevated temperatures are still scarce. The irradiation performance of fcc transition metal alloys with medium to high entropy have been widely studied, predominantly the NiCoFeCrM (M=Mn, Al, Cu and Pd) and the binary and ternary subsystems of NiCoFeCr [16]. For non-equiatomic systems, the ion irradiated microstructure evolution as a function of temperature has been studied by Kumar et al. [17] in Fe-28%Ni-27%Mn-18%Cr to 10 displacements per atom (dpa) at 400-700℃, and by Yang et al. [18] in $Al_{0.1}$CoCrFeNi to 31 dpa at 250-650℃. In both cases, the density of dislocation loops decreased while the loop size increased with increasing irradiation temperature. However, no voids were observed in both cases at all tested temperatures. In Kumar's study, the irradiation dose of up to 10 dpa may be too low for voids to be detected by their TEM analysis, given the good swelling resistance reported in HEAs. Additionally, the observation of stacking fault tetrahedra (SFT) by Yang [18] when irradiated at 500 and 650 ℃ to 31 dpa indicates that SFT may be the minimum energy form of vacancy clusters in $Al_{0.1}$CoCrFeNi in the temperature range, suggesting that void formation is unlikely.

The irradiation response of equiatomic NiCoFeCrMn and its subsystems irradiated at 500℃ has been studied using step-height measurements [14] and cross-sectional TEM observations [12-13]. Contrary to the case observed by Kumar and Yang, void-induced swelling was observed in all studied cases. However, the effect of compositional complexity on defect evolution, especially on voids, was only studied at a single irradiation temperature. Since the optimum void formation temperature ranges between 0.3-0.6 T_m, with T_m as the melting temperature of the material, more study on the temperature dependence of radiation tolerance of these alloys is necessary. Furthermore, the size of the alloying elements in Ni concentrated binary alloys has been demonstrated to have profound influence on defect evolution [19], where Pd and Mn atoms drastically reduce the size of voids and dislocation loops. When evaluating the swelling behavior of HEAs, it is critical to include more than one material and more than one irradiation temperature.

In the current work, the most studied HEA, NiCoFeCrMn and the recently developed NiCoFeCrPd (denoted by Mn-HEA and Pd-HEA, respectively hereafter) were chosen to study swelling behavior as a function of temperature. Both HEAs are equiatomic solid solution alloys. The elemental metals Ni, Co, Fe, Cr, Mn and Pd (> 99.9% pure) were carefully weighed and mixed by arc melting. The arc-melted buttons were flipped and re-melted at least five times before drop casting to ensure homogeneous mixing. The ingots were homogenized for 24 hours at 1200 °C, and then rolled at room temperature in steps to a final thickness of ~1.8 mm. The rolled specimens were annealed at 1170 °C for several days. Materials show equiaxed grain structures with an averaged grain size of a few hundreds of μm for both HEAs to minimize the effect from grain boundaries. The material properties of the chosen alloys are summarized in Table 1. The Mn and Pd atoms have an atomic volume size factor of 23.2 % and 41.3% compared to Ni [20], respectively.

Prior to irradiation, all the samples were chemical-mechanically polished to achieve a mirror-like finish surface with roughness of less than 3 nm. The samples were irradiated with 3 MeV Ni^{2+} ions to three temperatures, i.e. 420, 500 and 580°C, under a vacuum of 5×10^{-5} Pa to a fluence of $5.0 \times 10^{16} cm^{-2}$ at the Ion Beam Materials Lab (IBML) at the University of

Tennessee, Knoxville [21]. The flux was controlled at $2.8 \times 10^{12}\ ions/cm^2 s$. The irradiation temperatures were ~0.45, 0.5 and $0.55T_m$ for both alloys. An irradiation temperature of 675°C ($0.61T_m$) was performed on Mn-HEA to test the range of swelling temperature, but no voids were observed. A defocused beam was wobbled to achieve uniform irradiation, with scanning frequencies of 517 and 64 Hz for the horizontal and vertical direction, respectively. The irradiation induced damage profile and injected ion concentration were calculated using SRIM-2013 in Quick Kinchin-Pease Mode with a displacement threshold energy of 40 eV for all elements. The results of the calculations are plotted in Fig. S1.

The preparation of TEM samples and the electron microscopy characterization were conducted at the Michigan Center for Material Characterization at the University of Michigan (MC^2). Cross-sectional TEM samples were prepared using the focused-ion beam (FIB) lift-out technique on a FEI Helios Nanolab workstation. Prior to imaging dislocation loop features, a flash polishing technique [9] was applied on Mn-HEA to remove defects induced by FIB preparation, while a low energy ion cleaning method was applied on Pd-HEA. The final thickness of the sample was measured using the electron energy loss spectroscopy (EELS) method, the final specimen thickness ranged between 100 and 150 nm. Characterization of irradiation-induced defects were conducted using a JEOL 3011TEM with under-focused conditions in bright field (BF) and JEOL 2100 STEM in high angle annular dark field (HAADF).

Fig. 1 shows the cross-sectional BF images of Mn-HEA and Pd-HEA irradiated at the three temperatures. Voids were observed in all conditions, with average void size increasing with increasing temperature. It is challenging to select a certain depth region for swelling analysis due to the wide ranged void distribution across various temperatures. Instead, the voids observed at a depth up to 1800nm were taken into consideration when discussing swelling behavior. The depth was selected to be consistent with previous studies [12-14]. Table 2 summarizes the average void size, void number density, and total swelling for all voids observed within 1800 nm from the surface. In Mn-HEA irradiated at 580℃, a few large voids observed beyond 1800nm were not taken into consideration, but their effect toward total swelling is insignificant. At least two samples were counted for HEAs irradiated at 580℃ to ensure better statistics. Void swelling was calculated as the ratio of the volume of observed voids to the total sample volume analyzed.

The temperature dependent swelling behavior of two HEAs can be discussed in detail based on their irradiation temperatures. In general, Mn-HEA exhibited higher total swelling than Pd-HEA. At 420℃, the higher swelling observed in Mn-HEA than Pd-HEA is primarily due to higher void number density, and a slightly larger void size. At 500℃, Mn-HEA and Pd-HEA have similar total swelling, when taking the swelling uncertainties into consideration. However, the main contributor toward swelling is different. In this case, the void number density of Mn-HEA is ~ 4 times higher than Pd-HEA, despite the average void size of Pd-HEA being ~ 2 times larger than Mn-HEA. At 580℃, the swelling of Mn-HEA is higher than Pd-HEA due to the significantly increased void size (92.1 v.s. 67.0 nm) as temperature increased. The contribution from changes in void size in Mn-HEA outweighed the contribution from an order higher of void number density observed in Pd-HEA. The total swelling of the two HEAs is plotted in Fig. 2. The swelling trend indicates that at 420 ℃(~$0.45T_m$), the void growth is restricted due to low vacancy mobility. It is also reasonable to derive that for irradiation temperatures lower than 420℃, voids are unlikely to form for both tested HEAs up to 60 dpa at peak damage, given the

small, isolated voids observed in the current condition.

At least an order higher of swelling increase was observed in both HEAs when increasing irradiation temperature from 0.45 to $0.55T_m$. Furthermore, the average void size increased in both HEAs with increasing temperature. However, Pd-HEA seemed to have a stronger effect in suppressing void growth than Mn-HEA. The increment of void growth with changing temperatures is not as pronounced as the case in Mn-HEA. This stronger suppression is attributed to higher lattice distortion in Pd-HEA and stronger binding energy between vacancies and atoms with larger atomic size. The former has been demonstrated by Tong [22] using X-ray total scattering, while the latter has been observed by Yang [19] in Ni-20Pd and Ni-20Mn. Both interactions can effectively restrict the vacancy mobility, promote a higher recombination rate between vacancies and interstitials, leaving less free point defects and eventually lead to smaller void swelling, as shown in [23]. The dose dependence of swelling is not performed in this study. However, if a higher dose experiment is conducted in the future, the swelling trend is predicted as follows: the larger the atomic size of alloying elements involved in solid solution alloys, the further the incubation period for void nucleation can be prolonged, and the void growth will be further suppressed, similar to the result observed by Kato et al. [24].

One unique feature of using ion irradiation is the depth dependent information related to the irradiation direction. The depth dependent void distribution can provide insights into understanding defect mobility and interactions with increasing temperature. The representative features are harder to capture in TEM images as the voids become larger and the number density drops with increasing temperature. Fig. 3 shows the cross-sectional HAADF STEM images of two HEAs irradiated at 580℃. Contrary to the BF TEM images, voids appear as black circles here due to the lack of mass in the voided area when imaged using atomic mass contrast. Based on the HAADF images, one can observe distinguished void distributions between two HEAs. In Mn-HEA, voids are constantly distributed beyond the 1000 nm depth from the surface across three irradiation temperatures. Furthermore, the overall distribution region widens as vacancy mobility is increased with increasing temperature. While in Pd-HEA, at 420℃, only isolated voids were observed beyond 1000 nm. As irradiation temperature increased to 500℃, voids were observed not only in the region beyond 1000 nm, but in the main irradiation damage region (<1000 nm) as well. The distribution trend holds true when temperature increased to 580℃, with no significant extension of the distribution region. This indicates that the increase of vacancy mobility is not as pronounced in Pd-HEA than Mn-HEA. For Pd-HEA, the coexistence of large voids and high density dislocation loops in the main irradiation damage region is contrary to the solute trapping effect on defects. Previous theory [23] suggests added solute atoms (or increase lattice distortion) can effectively increase the recombination rate between vacancies and interstitials by trapping point defects. In that sense, Pd-HEA should have better swelling resistance than Mn-HEA in this region, but that was not the case. One potential explanation for the co-existence of voids and high density dislocation loops may be a smaller nucleation rate difference between vacancies and interstitials [24] in Pd-HEA. Combining with a stronger binding energy between alloying elements and defects, both defects were allowed to grow simultaneously. Further simulation work is desired to thoroughly investigate the interaction between irradiation induced defects.

The evolution of dislocation loops with increasing temperature is presented here. Fig. 4

shows the cross-sectional TEM images of dislocation loops in two HEAs for all tested conditions. The dislocation loops were imaged near g=[200] two beam condition. The size of the dislocation loops was consistently smaller and with higher loop density in Pd-HEA than Mn-HEA. Despite adapting two different cleaning methods, the main irradiation damage region can still be clearly distinguished. For Mn-HEA, as temperature increases to 580℃, the dominating feature shifts from small dislocation loops to tangled dislocation line segments. While in Pd-HEA, small dislocation loops remain to be the main defect feature. The pronounced delay in dislocation loop growth can be attributed and viewed as direct proof to the limited interstitial mobility arising from higher lattice distortion in Pd-HEA than Mn-HEA. The mobility of interstitials can be more effectively retarded when alloying with elements with larger atomic size differences, i.e. Pd [19, 25-26].

When irradiating samples at elevated temperatures for a higher dose, the annealing effect should be also taken into consideration. Despite that no secondary phase or phase decomposition was observed in this study, other previous studies have showed a formation of secondary phases in Mn-HEA during the annealing process. For instance, Otto et al. [27] observed intricate chemical decomposition in Mn-HEA, where most of the decomposition formed along grain boundaries after 500 days of annealing at 500℃ and 700℃, but not the case annealed at 900℃. Pickering et al. [28] further confirmed that no secondary phase formed at grain boundaries for Mn-HEA aged at 700℃ for less than 500 hours. This indicates that prolonged annealing for at least hundreds of hours is required for the formation of secondary phases in coarse grained Mn-HEA (with a grain size of hundreds of microns), and potentially even longer for annealing temperatures lower than 700℃ to reach thermal equilibrium. While in our case, irradiated samples were only exposed to elevated temperature for about 5 hrs during the whole irradiation process. The relatively short irradiation time may be one of the reasons why secondary phases were not observed in our study. The reported L10 (NiMn)-type ordering decomposition and <001> oriented spinodal decomposition between Co/Ni and Pd observed by Mo-Rigen [29] using electron irradiation was not found in our ion irradiated HEAs either. The lack of decomposition structure can potentially be attributed to the far from equilibrium states generated by ion irradiation than electron irradiation, which may make the role of mixing enthalpy (a likely contributor to decomposition [29]) much less relevant.

In this study, we demonstrate the superior swelling resistance in the equiatomic Ni-based HEAs over three irradiation temperatures. Despite an order of magnitude increase on swelling with increasing temperature, the highest total swelling in Mn-HEA is still below 0.5%. Combining the results of average size, number density of voids, and the evolution of dislocation loops, it is concluded that the better swelling resistance arises from the complex arrangement of different atomic species in HEAs. This arrangement gives rise to a highly-distorted lattice, a higher migration barrier for both defects and stronger solute-vacancy binding. The increase of equilibrium vacancy concentration in HEAs [30] may also contribute to the low overall swelling, making void saturation more difficult as temperature increases. Between the two HEAs studied, our results demonstrate that alloying with Pd can more effectively delay the growth of dislocation loops than alloying with Mn. Pd-HEA also shows stronger suppression effect on void growth at higher temperatures.

Acknowledgements

The work was supported as part of the Energy Dissipation to Defect Evolution (EDDE), an Energy Frontier Research Center funded by the US Department of Energy, Office of Science, Basic Energy Sciences. Ion beam work was performed at the University of Tennessee-Oak Ridge National Laboratory Ion Beam Materials Laboratory (IBML) located on the campus of the University of Tennessee-Knoxville. Cross-sectional TEM was conducted in the Michigan Center for Material Characterization of the University of Michigan.

References

[1] J.W. Yeh, S.K. Chen, S.J. Lin, J.Y. Gan, T.S. Chin, T.T. Shun, C.H. Tsau, S.Y. Chang, Adv. Eng. Mater. 6 (2004) 299.
[2] A. Gali, E.P. George, Intermetallics, 39 (2013) 74.
[3] F. Otto, A. Dlouhý, C. Somsen, H. Bei, G. Eggeler, E.P. George, Acta Mater, 61 (2013) 5743. doi:10.1016/j.actamat.2013.06.018.
[4] Z. Wu, H. Bei, G.M. Pharr, E.P. George, Acta Mater, 81 (2014) 428. doi:10.1016/j.actamat.2014.08.026
[5] G. Velişa, E. Wendler, S. Zhao, K. Jin, H. Bei, W.J. Weber, Y. Zhang, *Mater. Res. Lett*. 6 (2017) 136. doi: 10.1080/21663831.2017.1410863
[6] Y. Zhang, S. Zhao, W.J. Weber, K. Nordlund, F. Granberg, F. Djurabekova, Curr. Opin. Solid State Mater. Sci. 21 (2017) 221. doi:10.1016/j.cossms.2017.02.002.
[7] K. Jin, W. Guo, C. Lu, M.W. Ullah, Y. Zhang, W.J. Weber, L. Wang, J.D. Poplawsky, H. Bei, Acta Mater. 121 (2016) 365. doi:10.1016/j.actamat.2016.09.025.
[8] G. Velisa, M.W. Ullah, H. Xue, K. Jin, M.L. Crespillo, H. Bei, W.J. Weber, Y. Zhang, Acta Mater. 135 (2017) 54. doi:10.1016/j.actamat.2017.06.002.
[9] C. Lu, K. Jin, L.K. Béland, F. Zhang, T. Yang, L. Qiao, Y. Zhang, H. Bei, H.M. Christen, R.E. Stoller, L. Wang, Sci. Rep. 6 (2016) 19994. doi:10.1038/srep19994.
[10] E. Levo, F. Granberg, C. Fridlund, K. Nordlund, F. Djurabekova, J. Nucl. Mater. 490 (2017) 323. doi:10.1016/j.jnucmat.2017.04.023.
[11] Y. Zhang, G. M. Stocks, K. Jin, C. Lu, H. Bei, B. C. Sales, L. Wang, L. K. Béland, R. E. Stoller, G. D. Samolyuk, M. Caro, A. Caro, and W. J. Weber, Nat. Commun. 6 (2015) 8736. doi: 10.1038/ncomms9736 (2015).
[12] C. Lu, L. Niu, N. Chen, K. Jin, T. Yang, P. Xiu, Y. Zhang, F. Gao, H. Bei, S. Shi, M. He, I.M. Robertson, W.J. Weber, L. Wang, Nat. Commun. 7 (2016) 13564. doi:10.1038/ncomms13564.
[13] T. Yang, C. Lu, K. Jin, M.L. Crespillo, Y. Zhang, H. Bei, L. Wang, J. Nucl. Mater. 488 (2017) 328. doi:10.1016/j.jnucmat.2017.02.026.
[14] K. Jin, C. Lu, L.M. Wang, J. Qu, W.J. Weber, Y. Zhang, H. Bei, Scr. Mater. 119 (2016) 65. doi:10.1016/j.scriptamat.2016.03.030.
[15] S. Shi, H. Bei, I.M. Robertson, Mater. Sci. Eng. A. 700 (2017) 617. doi: 10.1016/j.msea.2017.05.049.
[16] K. Jin, H. Bei, Front. Mater. 5 (2018) 26. doi:10.3389/fmats.2018.00026.
[17] N.A.P. Kiran Kumar, C. Li, K.J. Leonard, H. Bei, S.J. Zinkle, Acta Mater. 113 (2016)

230. doi: 10.1016/j.actamat.2016.05.007.
[18] T. Yang, S. Xia, W. Guo, R. Hu, J.D. Poplawsky, G. Sha, Y. Fang, Z. Yan, C. Wang, C. Li, Y. Zhang, S.J. Zinkle, Y. Wang, 144 Scr. Mater. (2018) 31. doi: 10.1016/j.scriptamat.2017.09.025.
[19] T. Yang, C. Lu, G. Velisa, K. Jin, P. Xiu, M. Crespillo, Y. Zhang, H. Bei and L. Wang, Acta Materialia, 151 (2018) 159. doi: 10.1016/j.actamat.2018.03.054.
[20] H.W. King, J. Mater. Sci. 1 (1966)79.
[21] Y. Zhang, M. L. Crespillo, H. Xue, K. Jin, C.-H. Chen, C. L. Fontana, J. T. Graham, W. J. Weber, Nucl. Instrum. Meth. B 338 (2014) 19. doi:10.1016/j.nimb.2014.07.028.
[22] Y. Tong, G. Velisa, S. Zhao, W. Gao, T. Yang, K. Jin, C. Lu, H. Bei, J.Y.P. Ko, D.C. Pagan, Y. Zhang, L. Wang, F.X. Zhang, J. Mtla. (2018) in press. doi:10.1016/j.mtla.2018.06.008.
[23] L.K. Mansur and M.H. Yoo, J. Nucl. Mater. 74 (1978) 228.
[24] T. Yoshiie, M. Kiritani, J. Nucl. Mater. 271-272 (1999) 296.
[25] T. Kato, H. Takahashi and M. Izumiya, Mater. Trans. 32 (1991) 921.
[26] S. Shi, M. He, K. Jin, H. Bei and I. Robertson, J. Nucl. Mater. 501 (2018)132.
[27] F. Otto, A. Dlouhy, K.G. Pradeep, M. Kubenova, D. Raabe, G. Eggeler, E.P. George, Acta Mater. 112 (2016) 40. doi:10.1016/j.actamat.2016.04.005.
[28] E.J. Pickering, R. Munoz-Moreno, H.J. Stone, N.G. Jones, Scr. Mater. 113 (2016) 106. doi:10.1016/j.scriptamat.2015.10.025.
[29] M. He, S. Wang, S. Shi, K. Jin, H. Bei, K. Yasuda, S. Matsumura, K. Higashida, I.M. Robertson, Acta Mater. 126 (2017) 182. doi:10.1016/j.actamat.2016.12.046.
[30] Z. Wang, C.T. Liu, P. Dou, Phys. Rev. Mater. 1 (2017) 043601. doi:10.1103/PhysRevMaterials.1.043601

Table 1 Summary of material properties of NiCoFeCrMn and NiCoFeCrPd.

Material	Lattice parameter (Å)	Melting temperature (K)	$0.45T_m$ (℃)	$0.50T_m$ (℃)	$0.55T_m$ (℃)
NiCoFeCrMn	3.599	1553	425.9	503.5	581.2
NiCoFeCrPd	3.673	1560	429.0	507.0	585.0

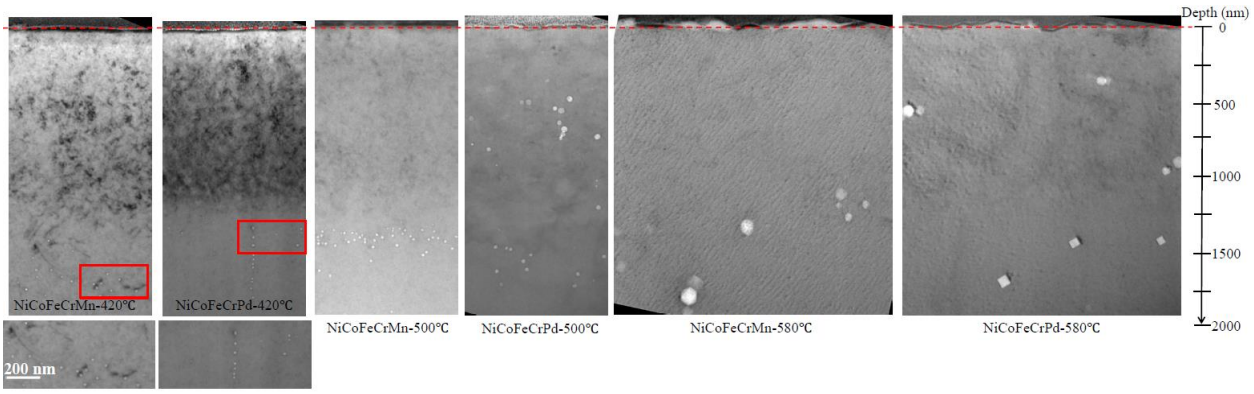

Figure 1. Cross-sectional BF TEM images of Mn-HEA and Pd-HEA irradiated by 3.0 MeV Ni^{2+} ions to $5 \times 10^{16} cm^{-2}$ at 420, 500 and 580℃. The enlarged areas were marked in red to help identify the relative location. For the actual scale, please refer to the scale bar under image or on the side.

Table 2. Summary of voids in 3 MeV Ni^{2+} irradiated Mn-HEA and Pd-HEA in the region of 0-1800 nm from surface, with irradiation temperature as 420, 500 and 580℃.

Materials	Temperature (℃)	Average void size (nm)	Void number density (10^{20} m^{-3})	Total swelling (%)
NiCoFeCrMn	420	13.2±1.1	1.09±0.11	0.015±0.004
	500	14.4±1.1	3.84±0.38	0.072±0.022
	580	92.1±3.7	0.05±0.005	0.37±0.044
NiCoFeCrPd	420	8.8±0.9	0.60±0.06	0.0026±0.001
	500	24.2±1.5	0.98±0.10	0.10±0.017
	580	67.0±2.6	1.60±0.16	0.29±0.046

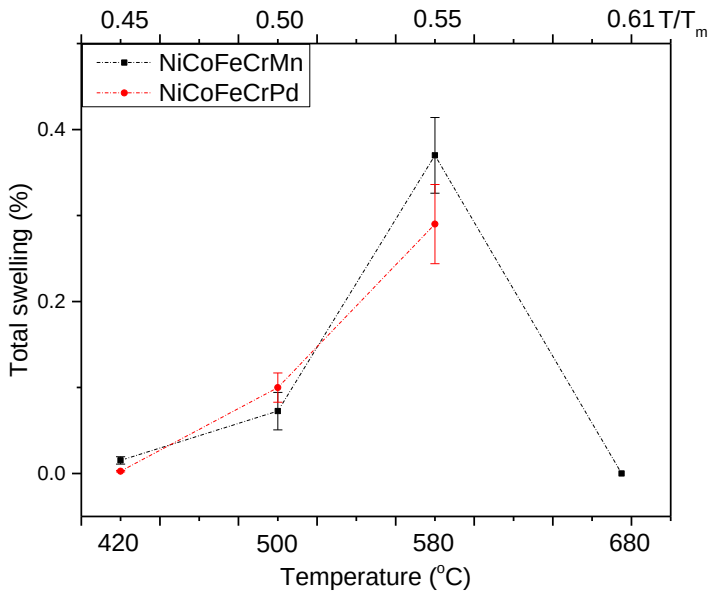

Figure 2. Temperature dependence of overall swelling in Mn-HEA and Pd-HEA irradiated by 3.0 MeV Ni^{2+} ions to $5 \times 10^{16} cm^{-2}$. Dotted lines are for guidance.

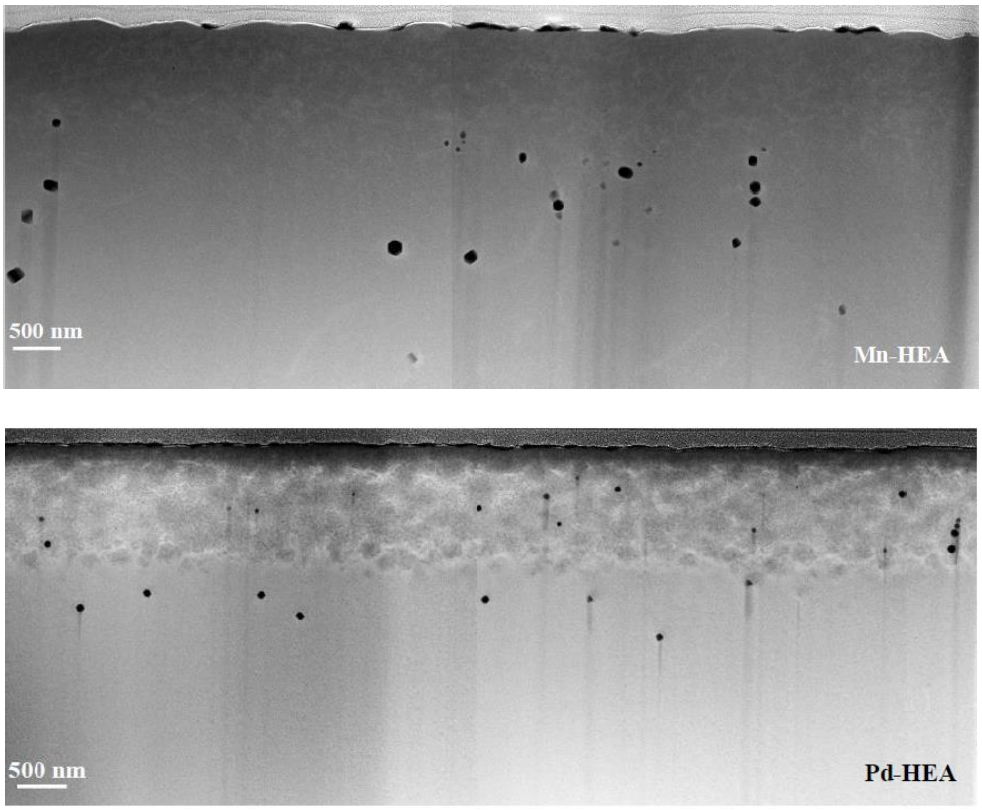

Figure 3. Cross-sectional HAADF STEM images of Mn-HEA and Pd-HEA irradiated by 3.0 MeV Ni^{2+} ions to $5 \times 10^{16} cm^{-2}$ at 580℃.

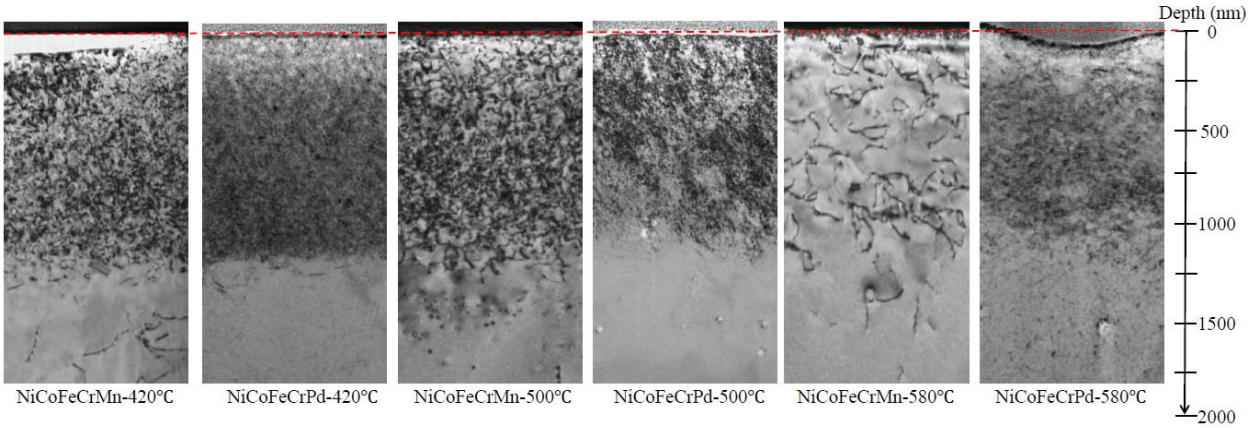

Figure 4. Distribution of dislocation loops at under-focus cross-sectional BF TEM images of Mn-HEA and Pd-HEA irradiated by 3.0 MeV Ni^{2+} ions to $5 \times 10^{16} cm^{-2}$ at 420, 500 and 580℃.

Appendices

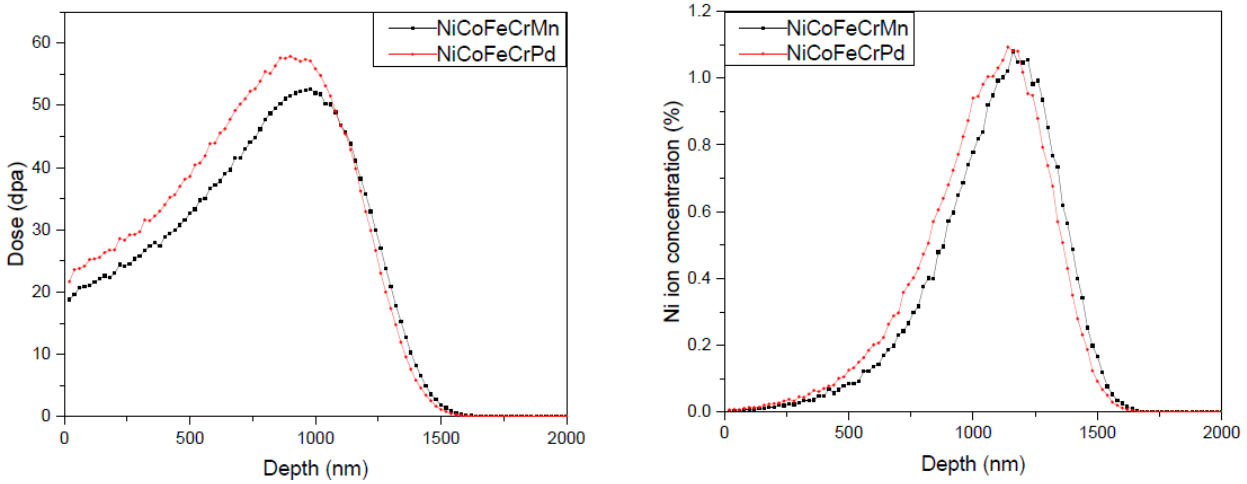

Fig. S1. SRIM prediction profile of depth distribution of (a) displacement damage and (b) implanted ions for 3.0 MeV Ni^{2+} ions irradiated to $5 \times 10^{16} cm^{-2}$.